
Pro-tuning: Unified Prompt Tuning for Vision Tasks

Xing Nie^{1,2}, Bolin Ni^{1,2}, Jianlong Chang³, Gaomeng Meng^{1,2,4}, Chunlei Huo^{1,*},
Zhaoxiang Zhang^{1,4}, Shiming Xiang¹, Qi Tian³, Chunhong Pan¹

¹ National Laboratory of Pattern Recognition, Institute of Automation, Chinese Academy of Sciences.
² School of Artificial Intelligence, University of Chinese Academy of Sciences. ³ Huawei Cloud & AI.
⁴ CAS Centre for Artificial Intelligence and Robotics, HK Institute of Science and Innovation.
 Email: niexing2019@ia.ac.cn, {gfmeng, clhuo}@nlpr.ia.ac.cn

Abstract

In computer vision, fine-tuning is the de-facto approach to leverage pre-trained vision models to perform downstream tasks. However, deploying it in practice is quite challenging, due to adopting parameter inefficient global update and heavily relying on high-quality downstream data. Recently, prompt-based learning, which adds a task-relevant prompt to adapt the downstream tasks to pre-trained models, has drastically boosted the performance of many natural language downstream tasks. In this work, we extend this notable transfer ability benefited from prompt into vision models as an alternative to fine-tuning. To this end, we propose parameter-efficient **Prompt tuning** (Pro-tuning) to adapt frozen vision models to various downstream vision tasks. The key to Pro-tuning is prompt-based tuning, *i.e.*, learning task-specific vision prompts for downstream input images with the pre-trained model frozen. By only training a few additional parameters, it can work on diverse CNN-based and Transformer-based architectures. Extensive experiments evidence that Pro-tuning outperforms fine-tuning in a broad range of vision tasks and scenarios, including image classification (generic objects, class imbalance, image corruption, adversarial robustness, and out-of-distribution generalization), and dense prediction tasks such as object detection and semantic segmentation.

1 Introduction

Fine-tuning is the dominant technique for using pre-trained vision models to perform downstream tasks, which has contributed towards significant advances in a wide variety of computer vision problems [2; 30; 34; 35; 47; 49]. Its standard practice is first to pre-train a general-purpose model on a large-scale dataset (*e.g.*, ImageNet [9]), then fine-tune the entire pre-trained model on downstream tasks. Although the achievements in the literature are brilliant, the fine-tuned model is still quite intractable to handle practical downstream vision applications for two main reasons. First, it requires updating and storing all model parameters separately for each downstream task, which is prohibitively expensive for the current ever-increasing vision model capacity. Second, its effectiveness heavily relies on high-quality downstream data, however, realistic data encountered in practical scenarios probably contains various negative distractors. In Figure 1, we provide an empirical study of fine-tuning along with other popular tuning strategies. Though achieving decent accuracy on CIFAR-100 [24], fine-tuning encounters devastating damages on various pre-trained vision models under distribution perturbations, *e.g.*, more than 12% validation accuracy drop on long-tailed CIFAR-100 [5] with imbalanced ratio 100 over their performances on the original CIFAR-100.

Recently, prompt-based learning has made waves in the natural language processing (NLP) community by demonstrating astounding transfer performance on myriad downstream tasks [3; 12;

*Corresponding author.

38; 41; 42; 45; 46]. Typically, prompt is a task-relevant description prepended to the downstream input to induce the downstream task to the pre-trained model. Its key idea is to reformulate the downstream task aided by an appropriate prompt design, making it close to those solved during the original pre-training, rather than fine-tuning pre-trained models to adapt to downstream tasks. Following this ideology, vision-language pre-training [20; 21; 40; 58] has been gradually developed to put visual categories into a text input as prompt, in order to diametrically generate visual concepts from natural language. Though achieving remarkable performance on many downstream vision tasks even without fine-tuning the language model, their prompt tuning strategies are tailored for the multimodal model, inapplicable to the pre-trained vision model. A question naturally arises: can we devise a lightweight prompt tuning paradigm specifically for the pre-trained vision models to boost downstream vision tasks?

In this spirit, we introduce *Pro-tuning*, a unified tuning paradigm for a variety of vision models, including convolutional neural networks (CNNs) and vision transformer models. The key to Pro-tuning is prompt-based tuning, *i.e.*, only learning task-specific vision prompts for downstream input images while freezing the pre-trained vision model. Specifically, Pro-tuning constructs lightweight prompt blocks to generate task-specific discriminative prompts for each downstream input image. By blending intermediate feature maps of each input with the learned prompts, Pro-tuning can generate a compact and robust downstream model to adapt tuning demands on various vision tasks, while only training lightweight additional parameters per downstream task.

We demonstrate that Pro-tuning is a generic tuning framework for CNN-based and Transformer-based vision models, which can surpass fine-tuning on various recognition tasks of object detection, semantic segmentation, and image classification under a variety of practical scenarios, including generic objects, class imbalance, image corruption, adversarial robustness, and out-of-distribution generalization. Figure 1 illustrates the quantitative results of Pro-tuning and other tuning paradigms on two image classification datasets. In particular, on the original CIFAR-100 [14], Pro-tuning achieves a superior result compared with fine-tuning under DeiT-B [47], which brings in a significant gain of +1.0% validation accuracy with only 27.1x fewer trainable parameters. On the more challenging long-tailed CIFAR-100 [5] with imbalanced ratio 100, Pro-tuning brings +0.6% and +2.1% validation accuracy gains over fine-tuning under Swin-S [34] and ResNet-101 [13], which reduces the trainable parameters by up to 31x and 11x, respectively. Regarding object detection, the proposed Pro-tuning obtains comparable performance to full fine-tuning (42.3 AP *v.s.*, 42.2 AP) under HTC [6] on COCO val2017 while reducing the trainable parameters by 25.5% (80.0M *v.s.*, 60.4M). On ADE20K semantic segmentation, it brings +0.6 mIoU gains (41.3 mIoU *v.s.*, 40.7 mIoU) over full fine-tuning under UperNet [50] with the significant reduction of trainable parameters by 29.9% (46.6M *v.s.*, 66.5M).

The key contributions can be summarized as follow:

- A parameter-efficient vision tuning paradigm, *i.e.*, Pro-tuning, is proposed. This prompt-based tuning specifically for vision models can adapt frozen pre-trained models to downstream tasks with broad distributions.
- The proposed Pro-tuning can cooperate with various vision models including CNNs and vision transformers. As a plug-and-play technique, it is a capable general-purpose tuning framework with minor additional computational costs.
- Extensive experiments demonstrate that Pro-tuning exceeds fine-tuning on sixteen challenging benchmarks across three vision tasks, including image classification under five scenarios, and dense prediction tasks such as object detection and semantic segmentation.

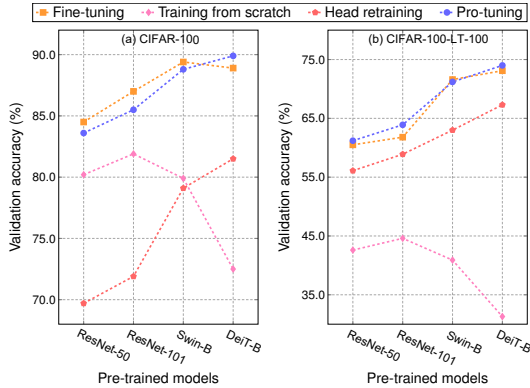


Figure 1: Comparison between the proposed Pro-tuning and other tuning paradigms under various pre-trained vision models. CIFAR-100-LT-100: Long-tailed CIFAR-100 with imbalanced ratio 100.

2 Related Work

2.1 Model Fine-Tuning

In computer vision, a series of techniques have been proposed to adapt general-purpose vision models to downstream tasks [7; 27; 52; 53; 54; 55]. However, the dominant techniques are still fine-tuning the entire moderately-sized pre-trained vision model (*e.g.*, ResNet [13] and DeiT-B [47]) on the downstream data. Recently, fine-tuning techniques have enabled remarkable progress in the NLP community [17; 32; 39; 44]. Notably, the flagship systems like GPT-3 [3] (composed of 175B parameters) achieve remarkable performance across a wide range of downstream tasks even without requiring additional task-specific parameters. Recent work [23; 40; 48; 54] empirically validates that larger pre-trained models have a tendency to achieve better transfer performance, thus an important ingredient in leading to such difference between computer vision and NLP could be the evident increasing scale of the pre-trained language model. In this work, we develop a parameter-efficient tuning paradigm for substantially exploiting the knowledge in frozen pre-trained vision models. Our focus is on exploring how far we can push without the advantages of large-scale pre-trained models.

2.2 Prompt-based Learning

Prompt-based learning [33] is proposed and fueled by the GPT series [3; 41; 42] in the field of NLP. This is an approach of adding task-relevant descriptions to the downstream input to help the pre-trained model understand the downstream tasks, rather than only adapting the pre-trained model to downstream tasks by fine-tuning. GPT-3 pioneers this route by treating each downstream task as a masked language modeling problem, where the model directly generates a textual response in prompt. Subsequently, numerous researches are devoted to devising efficient prompt strategies for mining knowledge from pre-trained language models [25; 12; 28; 45; 46]. Motivated by GPT-3, vision-language models such as CLIP [40] and ALIGN [20] diametrically generate vision concepts from natural language by training a large contrastive learning model over a large number of image-text pairs, where the key is to place visual categories into a text input as prompt. They achieve impressive performance on a wide range of vision tasks without any fine-tuning. However, prompt-based tuning methods in vision-language models are tailored for the multimodal model, and inapplicable to the pre-trained vision model. To fill this gap, our work aims to develop a parameter-efficient prompt tuning paradigm specifically for vision models, in order to adapt the frozen pre-trained vision model to downstream tasks on a broad distribution.

3 Pro-tuning

In this section, we describe the integration of Pro-tuning into pre-trained vision models with diverse network architectures, including CNNs and vision transformer models.

3.1 Overall Architecture

Pro-tuning is a method for adapting a pre-trained vision model to downstream tasks without changing its weight. To this end, we introduce lightweight prompt blocks to learn task-specific prompts for each downstream input, while freezing the pre-trained model. Inspired by studies [19; 29; 53], feature representations of different levels contribute to the generalization performance of the network, especially for low-level and mid-level representations. To sufficiently exploit semantic information from diverse levels to enrich the feature space, we build multiple stage-wise prompt blocks, which can be simply plugged into a given frozen pre-trained vision model for quickly adapting to a new task. Specifically, this process can be computed through four simple steps: 1) feeding each downstream input image into the frozen pre-trained model; 2) adopting intermediate feature maps from different stages to train stage-wise prompt blocks for producing prompts; 3) blending the learned prompts with the corresponding feature maps as input to the next stage of the frozen pre-trained model; 4) appending a fully-connected layer to top layers of the pre-trained model for the final prediction. In this way, the task-specific vision prompts can be obtained, maximally mitigating the gap between pre-training and tuning on downstream tasks. It is worth noting that vision models typically divide the whole network architectures into multiple sub-layers as stages, for either transformer-based or CNN-based models. To ensure the generality of our method, we follow their original concepts of stage partitioning. Intuitively, our Pro-tuning is illustrated in Figure 2.

Formally, consider a stage g_i of the n -stage pre-trained vision model $G = \{g_i\}_{i=1}^n$ and an input image \mathbf{x}^j on a downstream dataset $\mathcal{D} = \{(\mathbf{x}^j, \mathbf{y}^j)\}_{j=1}^{n_d}$, we define the multi-stage intermediate feature maps of \mathbf{x}^j as $\{\mathbf{x}_1^j, \mathbf{x}_2^j, \dots, \mathbf{x}_n^j\}$, thus the original network output \mathbf{x}_i^j after the stage g_i can be represented as $\mathbf{x}_i^j = g_i(\mathbf{x}_{i-1}^j)$. Suppose that each prompt block after stage g_i is represented by a function f_i , this prompt-based blending representation $\tilde{\mathbf{x}}_i^j$, with the intermediate feature map x_i^j and the learned task-specific prompt $f_i(x_i^j)$ aggregated, can be written as

$$\tilde{\mathbf{x}}_i^j = x_i^j + \beta \cdot f_i(x_i^j), \quad (1)$$

where β denotes a learnable parameter to balance the two terms. In this way, the task-specific knowledge of downstream data can be sufficiently distilled from different level representations. Note that, the prompt-based blending representation encourages a balance between the intermediate feature map and the learned prompt when pondering semantics of different stages, enabling adaptive control. Quite intuitively, our prompt blocks conducts a generic architectural modification to re-purpose a frozen pre-trained vision model for adapting to a downstream task via minor additional parameters. To this end, we implement each prompt block with three lightweight convolutional layers along with a SE module [18]: 1×1 convolution, 5×5 depthwise convolution [8], and 1×1 convolution. Our default setting is appending one prompt block after each stage. Further analysis about the number of prompt blocks and inserting positions can be referred to Sec. 4.4. Finally, an additional fully-connected layer h is appended to the top layer of pre-trained vision models for the network output. Details of configurations and stage partitioning can be found in the supplementary material.

3.2 Optimization

In our Pro-tuning, suppose the pre-trained vision model $G^{\phi_0} = \{g_i^{\phi_0}\}_{i=1}^n$ is parameterized by ϕ_0 , we define that all additional modules are parameterized by θ , including $\{f_i^\theta\}_{i=1}^n$ and h^θ . During training, we only update a few parameters θ with the pre-trained parameters ϕ_0 frozen. Our experiments show that updating ϕ and θ simultaneously hurts generalization in Sec 4.4, the reason could be attributed to the much fewer number of downstream images compared with the large-scale dataset used to pre-train ϕ . Training only the parameters θ makes our Pro-tuning *modular* – it can use an off-the-shelf pre-trained vision model removing the need for modifying

or re-training, merely adding a small number of additional parameters per task. It is applicable to the common scenario of cloud services, where a diverse set of downstream tasks need to be solved by a given vision model, thus this parameter sharing of frozen pre-trained models is significantly appealing. Thus, a parameter-efficient vision tuning paradigm, *i.e.*, Pro-tuning, can be formulated as

$$\theta^* = \arg \min_{\theta} \frac{1}{|\mathcal{D}|} \sum_{j=1}^{n_d} \ell \left(h^\theta(\tilde{\mathbf{x}}_i^j), \mathbf{y}^j \right),$$

$$\text{where } \tilde{\mathbf{x}}_i^j = g_i^{\phi_0}(\mathbf{x}_{i-1}^j) + \beta f_i^\theta \left(g_i^{\phi_0}(x_{i-1}^j) \right), \quad i = 2, \dots, n$$

$$\tilde{\mathbf{x}}_1^j = g_1^{\phi_0}(\mathbf{x}^j) + \beta f_1^\theta \left(g_1^{\phi_0}(\mathbf{x}^j) \right).$$
(2)

During training, we simply minimize the prediction error using the cross-entropy (CE) loss with the pre-trained model frozen. By only training a few additional parameters, the gradients can be back-propagated all the way through the pre-trained model, distilling the rich knowledge encoded in pre-trained parameters for learning the task-specific prompt.

4 Experiment

In this section, we systematically demonstrate the capability of the proposed Pro-tuning. First, we briefly introduce experimental settings in Sec 4.1. Then, we perform extensive experiments to validate

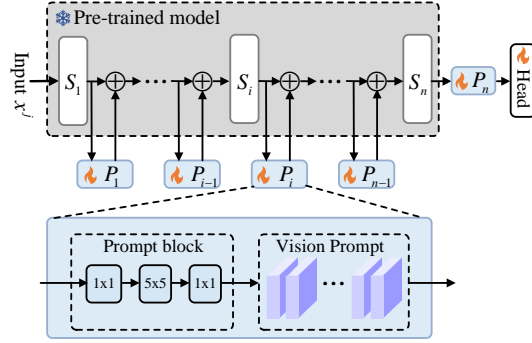


Figure 2: An overview of our proposed Pro-tuning.

Table 1: Details of the used downstream datasets.

Type	Dataset	Train size	Test size	#classes
Generic object	CIFAR-10 [24]	50,000	10,000	10
	CIFAR-100 [24]	50,000	10,000	100
	Clothing1M [51]	47,570	10,526	14
	Caltech-101 [26]	3,060	6,084	102
	Stanford Dogs [22]	12,000	8,580	120
	Oxford-IIIT Pets [37]	3,680	3,669	37
	Oxford 102 Flowers [36]	2,040	6,149	102
Class imbalance	CIFAR-10-LT-100 [5]	12,406	10,000	10
	CIFAR-10-LT-50 [5]	13,996	10,000	10
	CIFAR-100-LT-100 [5]	10,847	10,000	100
	CIFAR-100-LT-50 [5]	12,608	10,000	100
Image corruption	CIFAR-10-C [15]	-	950,000	10
	CIFAR-100-C [15]	-	950,000	100
Adversarial robustness	ImageNet-A [16]	-	7,500	200
Out-of-distribution Generalization	ImageNet-R [14]	-	30,000	200
Object detection	COCO [31]	118,287	5,000	80
Semantic segmentation	ADE20K [57]	20,210	2,000	150

Table 2: The performance of our proposed Pro-tuning and other tuning paradigms under three CNN-based pre-trained models on nine benchmarks. Notably, Params[†] denotes the maximum number of trainable parameters. “TS”: training from scratch, “HR”: head retraining, “FT”: fine-tuning.

Backbone	Method	Params [†]	C-10-LT		C-100-LT		C-10	C-100	PET	Flower	DOG	C1M	C-101
		(M)	IR100	IR50	IR100	IR50							
<i>CNN-based</i>													
ResNet-50	TS [54]	23.75	80.4	84.6	42.6	50.1	96.4	80.4	78.2	77.8	66.8	77.0	77.2
	HR [10]	0.25	83.6	85.0	56.1	60.2	86.1	69.7	91.8	93.0	88.9	66.5	90.0
	Partial-1 [53]	4.71	86.5	88.9	57.9	62.0	95.5	79.3	93.2	96.8	87.4	75.3	91.5
	Partial-2 [53]	9.17	87.3	89.5	56.8	62.1	96.1	80.9	92.8	97.3	85.8	76.5	92.2
	FT [1]	23.75	89.7	92.0	60.5	65.7	97.7	84.5	92.5	98.3	86.5	78.7	93.4
	Pro-tuning	3.86	89.9	92.2	61.2	66.0	97.6	83.6	92.5	97.1	87.8	77.5	92.9
ResNet-101	TS [54]	42.75	80.4	84.6	44.6	50.6	97.1	81.9	77.7	78.0	69.0	77.8	77.4
	HR [10]	0.25	85.3	86.5	58.9	62.7	87.6	71.9	92.4	92.8	90.5	67.2	90.7
	Partial-1 [53]	4.71	87.2	89.7	59.5	63.9	95.5	80.2	93.6	96.8	89.5	75.3	92.4
	Partial-2 [53]	9.17	87.8	90.5	59.0	63.7	96.4	81.7	93.2	97.6	88.0	76.3	92.8
	FT [1]	42.75	90.8	92.7	61.8	67.2	98.2	87.0	93.7	98.4	87.9	78.5	93.7
	Pro-tuning	3.86	91.0	93.3	63.9	68.4	98.0	85.5	92.9	97.1	89.6	77.2	93.8
RegNetX-32	TS [54]	105.59	77.5	83.0	39.2	46.3	96.8	81.5	77.8	78.3	70.2	77.5	77.2
	HR [10]	0.30	83.4	84.5	55.1	59.6	86.6	71.4	93.4	94.3	95.0	69.7	91.7
	Partial-1 [53]	3.69	86.2	88.6	57.6	62.2	93.9	78.1	94.1	97.3	94.2	76.2	93.7
	Partial-2 [53]	10.05	86.2	88.6	57.6	62.2	94.7	78.7	94.5	97.4	94.1	75.6	93.6
	FT [1]	105.59	91.0	92.7	63.7	68.9	98.4	87.2	94.0	98.7	88.0	78.8	95.1
	Pro-tuning	5.91	91.2	92.8	62.0	67.7	97.8	84.4	94.3	97.9	93.1	77.9	94.1

Pro-tuning on image classification under five scenarios, including generic objects, class imbalance, image corruption, adversarial robustness, and out-of-distribution generation in Sec 4.2. Moreover, we evaluate Pro-tuning on dense prediction tasks such as objection detection and semantic segmentation in Sec 4.3. Finally, we provide detailed ablation studies to analyze Pro-tuning in Sec 4.4.

4.1 Experimental Setting

To exhaustively evaluate the proposed Pro-tuning, we perform detailed experiments on fifteen long-standing benchmarks. Details of the used visual datasets are listed in Table 1. For abbreviation in Table 2 and Table 3, “C-10-LT”: long-tailed CIFAR-10, “C-100-LT”: long-tailed CIFAR-100, “C-10”: CIFAR-10, “C-100”: CIFAR-100, “PET”: Oxford-IIIT Pets, “Flower”: Oxford Flowers-102, “DOG”: Stanford Dogs, “C1M”: Clothing1M, “C-101”: Caltech-101. We show that the proposed Pro-tuning facilitates a board range of vision tasks under seven advanced pre-trained models, including CNN-based and Transformer-based architectures: ResNet-50 [13], ResNet-101 [13], RegNetX-32G [43], DeiT-S [47], DeiT-B [47], Swin-S [34], Swin-B [34]. During training, we first use the pre-trained weights on ImageNet to initialize pre-trained vision models. In Table 2 and Table 3, we compute the

Table 3: The performance of our proposed Pro-tuning and other tuning paradigms under four Transformer-based pre-trained models on nine benchmarks. Notably, Params[†] denotes the maximum number of trainable parameters. “TS”: training from scratch, “HR”: head retraining, “FT”: fine-tuning.

Backbone	Method	Params [†]	C-10-LT		C-100-LT		C-10	C-100	PET	Flower	DOG	CIM	C-101
		(M)	IR100	IR50	IR100	IR50							
<i>Transformer-based</i>													
DeiT-S	TS [54]	21.71	58.9	67.9	33.5	37.9	95.3	74.1	41.8	68.9	34.4	68.4	50.1
	HR [10]	0.05	83.6	86.9	63.1	66.8	92.6	77.0	92.8	89.0	92.7	66.2	90.6
	Partial-1 [53]	1.23	87.7	89.2	62.2	66.5	95.6	80.9	93.6	92.7	92.6	70.9	91.5
	Partial-2 [53]	1.82	89.3	91.6	64.6	68.9	96.9	83.5	94.2	95.6	92.2	74.6	92.7
	FT [1]	21.71	92.0	94.0	69.4	73.6	98.5	87.5	93.8	98.3	87.5	78.5	94.8
	Pro-tuning	0.85	92.6	94.2	70.0	74.4	98.2	88.0	94.0	97.0	92.4	78.3	94.3
Swin-S	TS [54]	48.93	62.6	70.8	40.7	47.2	95.1	79.9	52.9	74.3	45.9	21.6	66.1
	HR [10]	0.09	83.5	87.6	61.9	66.4	93.3	78.4	93.3	88.8	95.0	66.5	91.6
	Partial-1 [53]	2.45	86.6	89.7	64.1	69.0	94.4	80.8	93.5	93.3	94.9	70.2	92.5
	Partial-2 [53]	4.82	90.2	92.2	65.3	70.2	96.8	84.6	94.9	95.9	94.8	76.0	93.5
	FT [1]	48.93	93.6	95.8	70.6	75.5	99.0	89.4	94.6	98.9	90.2	80.0	96.2
	Pro-tuning	1.54	93.8	95.5	71.2	75.3	98.6	88.7	95.0	97.0	94.5	78.4	94.7
DeiT-B	TS [54]	85.89	58.2	65.8	31.3	35.2	95.5	72.5	40.2	71.1	29.8	58.1	50.3
	HR [10]	0.09	87.5	90.3	67.3	71.4	95.1	81.5	93.6	93.0	96.0	69.9	91.8
	Partial-1 [53]	4.82	89.8	92.0	65.8	70.5	97.2	84.2	94.4	95.1	95.8	72.2	93.2
	Partial-2 [53]	7.18	91.7	93.7	69.2	73.8	98.1	87.2	94.8	96.8	95.6	76.1	93.9
	FT [1]	85.89	93.8	94.8	73.1	76.5	98.7	88.9	94.0	98.5	91.2	78.7	95.9
	Pro-tuning	3.17	93.5	95.5	74.0	77.7	98.8	89.7	94.7	97.7	95.9	78.5	95.6
Swin-B	TS [54]	86.87	62.3	70.1	40.9	46.9	94.8	79.5	44.8	76.7	5.2	19.6	67.4
	HR [10]	0.12	84.6	88.2	63.0	67.5	94.0	79.1	92.8	90.6	95.6	68.2	92.1
	Partial-1 [53]	4.32	86.5	89.4	64.3	68.7	94.8	81.0	93.6	94.2	95.5	71.4	92.5
	Partial-2 [53]	8.52	88.7	91.4	64.4	69.6	96.9	84.3	94.4	95.4	95.5	95.7	93.4
	FT [1]	86.87	93.9	95.3	71.6	76.2	98.5	89.4	95.1	98.9	91.8	79.9	96.5
	Pro-tuning	2.67	94.2	95.4	71.2	75.7	98.6	88.8	95.0	96.7	95.5	77.7	93.8

maximum number of trainable parameters to measure the parameter efficiency, denote by Params[†]. More experimental details can be referred to in the supplementary material.

To put our results in perspective, we compare the proposed Pro-tuning with a series of commonly used protocols, *i.e.*, 1) *fine-tuning* [1], which fine-tunes the weight of the pre-trained vision model while retraining the new head classifier on downstream tasks; 2) *partial fine-tuning* [53], which fine-tunes the last several layers of the pre-trained vision model while freezing the remaining parts and retraining a new head classifier on downstream tasks, including two variants *Partial-1* and *Partial-2* according to the number of trainable parameters; 3) *head retraining* [10], which retrains the head classifier while freezing the weight of the pre-trained model; 4) *training from scratch*, which trains the whole vision model from random initialization.

4.2 Image Classification

Class Imbalance Transferability. We conduct extensive experiments on the long-tailed CIFAR-10 and CIFAR-100 datasets. Table 2 and Table 3 show the results of Pro-tuning and other tuning paradigms. Under three pre-trained CNNs, Pro-tuning outperforms other tuning methods including fine-tuning (FT) and the most lightweight tuning method head retraining (HR) in most scenarios. Specifically, for long-tailed CIFAR-100 with imbalanced ratio 100, Pro-tuning achieves superior validation accuracy (63.9%) compared with fine-tuning (61.8%) and head retraining (58.9%) under ResNet-101 [13]. Regarding long-tailed CIFAR-10 with imbalanced ratio 50, Pro-tuning brings in 0.6% absolute accuracy improvement and reduces the trainable parameters by 91.0% compared with fine-tuning under ResNet-101 [13]. Under the larger-capacity RegNetX-32 [43], Pro-tuning also achieves superior performance (91.2% vs. 91.0%) over fine-tuning with a large reduction of trainable parameters by 94.4% on long-tailed CIFAR-10 with imbalanced ratio 100. For state-of-the-art transformer-based architectures, Pro-tuning also exhibits excellent performance. In particular, Pro-tuning consistently outperforms fine-tuning under DeiT-S [47] on various imbalanced ratios, with only 25.5x fewer trainable parameters. On long-tailed CIFAR-100 with imbalanced ratio 50, Pro-tuning brings in a gain of 1.2% validation accuracy over fine-tuning under DeiT-B [47] while reducing the trainable parameters by 96.3%. Moreover, compared with fine-tuning on long-tailed CIFAR-10 with imbalanced ratio 100 under Swin-S [34], Pro-tuning achieves superior validation accuracy using 31.8x fewer trainable parameters. Regarding Swin-B [34], Pro-tuning surpasses

fine-tuning on long-tailed CIFAR-10 with imbalanced ratio 50 and 100 with a large reduction of trainable parameters by 96.2%.

Generic Object Transferability. To reveal the transferability of generic objects, we report the quantitative results on seven downstream datasets with generic objects. As shown in Table 2 and Table 3, Pro-tuning shows remarkable performance under a series of pre-trained models. Specifically, Pro-tuning reaches the identical validation accuracy of fine-tuning under RegNetX-32 [43] on Oxford-IIIT Pets, while only using 17.9x fewer trainable parameters. Under three pre-trained CNNs, Pro-tuning brings in a gain of 9.8%~11.5% validation accuracy over head retraining on CIFAR-10 while obtaining comparable performances to fine-tuning. Moreover, Pro-tuning achieves superior validation accuracy with 11.1x trainable parameters over fine-tuning under ResNet-101 [13] on Caltech-101. For advanced transformer-based architectures, Pro-tuning achieves quite competitive performance compared with fine-tuning and head retraining. Specifically, Pro-tuning brings in 1.0% absolute accuracy improvement over fine-tuning with 27.1x fewer trainable parameters under DeiT-B on CIFAR-100. Moreover, Pro-tuning obtains superior performance (95.0% vs. 94.6%) than fine-tuning while reducing the trainable parameters by 96.9% under Swin-S [34] on Oxford-IIIT Pets. Under Swin-B [34], pro-tuning brings in a gain of 4.6% validation accuracy over head retraining and achieves comparable performance to fine-tuning with 32.5x fewer trainable parameters on CIFAR-10.

Image Corruption Robustness. We show the results on CIFAR-10-C and CIFAR-100-C in Table 4. Notably, our proposed Pro-tuning consistently performs better than all the other methods on two datasets under three pre-trained models. On CIFAR-10-C, our Pro-tuning brings in a gain of +0.4%~2.7% over fine-tuning, with only 6.5x~33.5x fewer trainable parameters. Compared with head retraining, Pro-tuning achieves better transfer performance with at least +10.5% absolute validation accuracy gains. On CIFAR-100-C, Pro-tuning brings +1.2% absolute validation accuracy gains than fine-tuning with more than 83.9% drop in trainable parameters (3.823M vs. 23.714M) under ResNet-50. The dramatic improvements demonstrate the capability of our proposed Pro-tuning to defend against image corruption.

Table 4: The performance of Pro-tuning and other tuning paradigms on CIFAR-10-C and CIFAR-100-C. “FT”: fine-tuning, “HR”: head retraining, “TS”: training from random initialization.

Backbone	Method	CIFAR-10-C		CIFAR-100-C	
		Params (M)	Top1 Acc. (%)	Params (M)	Top1 Acc. (%)
ResNet-50	FT [1]	23.532	80.8	23.714	57.4
	HR [10]	0.021	62.2	0.210	43.6
	TS [54]	23.532	83.0	23.714	58.2
	Pro-tuning	3.634	83.5	3.823	58.6
DeiT-S	FT [1]	21.670	91.1	21.704	72.8
	HR [10]	0.004	79.7	0.040	59.2
	TS [54]	21.670	85.9	21.704	59.1
	Pro-tuning	0.773	91.5	0.808	73.0
Swin-S	FT [1]	48.845	88.2	48.914	70.4
	HR [10]	0.008	79.7	0.080	59.1
	TS [54]	48.845	82.7	48.914	59.1
	Pro-tuning	1.458	90.2	1.527	70.7

Adversarial Robustness. We employ ImageNet-A to evaluate all the tuning methods on adversarial examples in Table 5. The performances of all tuning methods are relatively low on ImageNet-A, as this task is quite difficult. Even though, our Pro-tuning also outperforms other tuning methods under four advanced pre-trained models. For example, Pro-tuning surpasses fine-tuning with bringing in +4.8% absolute performance gains under DeiT-S, while requires only 25.7x fewer trainable parameters. Moreover, Pro-tuning brings in significant accuracy gains of +6.9% over fine-tuning with the reduction of trainable parameters by 96.7% under Swin-S.

Out-of-distribution Generalization. We present the validation accuracy and trainable parameters on ImageNet-R in Table 5. Note that the proposed Pro-tuning consistently surpasses head retraining under four pre-trained models. Specifically, Pro-tuning brings in a gain of +1.0% validation accuracy over fine-tuning using fewer trainable parameters under DeiT-S. Regarding the larger-capacity Swin-S, Pro-tuning obtains 46.2% validation accuracy, +1.2% higher than fine-tuning and head retraining.

Table 5: The performance of Pro-tuning and other tuning paradigms on ImageNet-A and ImageNet-R. “FT”: fine-tuning, “HR”: head retraining, “TS”: training from random initialization.

Backbone	Method	ImageNet-A		ImageNet-R	
		Params (M)	Top1 Acc. (%)	Params (M)	Top1 Acc. (%)
DeiT-S	FT [1]	21.743	15.6	21.743	40.6
	HR [10]	0.081	19.2	0.081	40.9
	TS [54]	21.743	6.5	21.743	24.9
	Pro-tuning	0.846	20.4	0.846	41.6
Swin-S	FT [1]	48.991	26.5	48.991	45.2
	HR [10]	0.154	32.8	0.154	45.2
	TS [54]	48.991	12.6	48.991	30.5
	Pro-tuning	1.604	33.4	1.604	46.4
DeiT-B	FT [1]	85.952	24.1	85.952	44.9
	HR [10]	0.154	27.8	0.154	44.0
	TS [54]	85.952	5.9	85.952	23.6
	Pro-tuning	3.236	28.5	3.236	44.3
Swin-B	FT [1]	86.948	33.6	86.948	47.4
	HR [10]	0.205	36.5	0.205	46.6
	TS [54]	86.948	13.7	86.948	30.3
	Pro-tuning	2.749	37.7	2.749	46.6

4.3 Dense Prediction

Object detection. We evaluate the proposed Pro-tuning over the object detection task under Cascade Mask RCNN [4] and HTC [6] with ImageNet pre-trained ResNet-50. As shown in Table 6, one can observe that our Pro-tuning achieves the comparable performance with the significant reduction of trainable parameters.

Table 6: Results of object detection on COCO2017 val set under Cascade Mask RCNN [4] and HTC [6] with ImageNet pre-training.

Methods	Params	Epochs	AP	AP ₅₀	AP ₇₅	AP _S	AP _M	AP _L
<i>Cascade Mask RCNN</i>								
Head retraining	53.8	12	34.2	52.9	36.8	19.3	36.9	45.7
Fine-tuning	77.1	12	41.2	59.4	45.0	23.9	44.2	54.4
Pro-tuning (ours)	57.4	12	41.1	60.6	44.9	24.3	43.5	55.5
<i>HTC</i>								
Head retraining	56.8	12	37.5	56.3	40.2	21.1	40.3	50.3
Fine-tuning	80.0	12	42.3	61.1	45.8	23.7	45.6	56.3
Pro-tuning (ours)	60.4	12	42.2	62.3	46.0	25.2	45.2	56.7

Semantic segmentation. To evaluate the semantic segmentation performance, we evaluate Pro-tuning under UperNet [50] and FCN [35] with ImageNet pre-trained ResNet-50. The results are shown in Table 7. One can observe that our Pro-tuning consistently outperform fine-tuning and head retraining.

4.4 Ablation Study

In this subsection, we conduct extensive ablation studies to systematically analyze the developed Pro-tuning with the ImageNet pre-trained ResNet-50 [13] and DeiT-B [47].

Analysis of few-shot learning. To evaluate the few-shot performance, we perform few-shot transfer by reducing the number of training examples on CIFAR-10, CIFAR-100, and Caltech-101 under ResNet-50. Following the representative few-shot protocol [11; 40; 58], we adopt 1, 2, 4, 8, and 16 shots for training and the full test sets for testing in Figure 3. One can observe that our Pro-tuning is a strong few-shot learner, requiring only 4 shots to

Table 7: Results of semantic segmentation on ADE20K val set under UperNet [50] and FCN [35] with ImageNet pre-training.

Backbone	Params	Steps	mIoU
<i>FCN</i>			
Head retraining	26.1M	80k	25.8%
Fine-tuning	49.6M	80k	35.9%
Pro-tuning (ours)	26.7M	80k	36.2%
<i>UperNet</i>			
Head retraining	43.0M	80k	38.7%
Fine-tuning	66.5M	80k	40.7%
Pro-tuning (ours)	46.6M	80k	41.3%

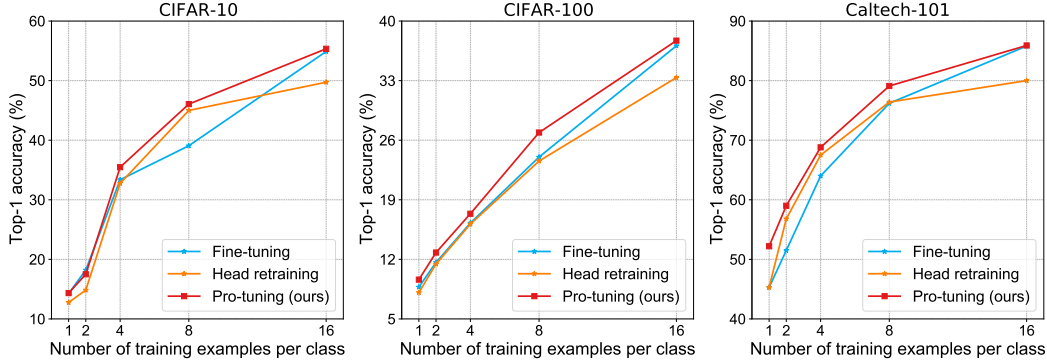


Figure 3: Results of few-shot learning under the ImageNet pre-trained ResNet-50 on the CIFAR-10, CIFAR-100, and Caltech-101 benchmarks.

obtain a significant margin with +2.1% absolute accuracy improvement over fine-tuning on CIFAR-10. Pro-tuning also achieves a superior result over head retraining and fine-tuning with 8 shots, which brings in +3.4% and +2.9% validation accuracy improvements on CIFAR-100. Moreover, Pro-tuning brings in a gain of 5.9% validation accuracy over head retraining with 16 shots on Caltech-101.

Integration with fine-tuning. To reveal the influence of different tuning settings, we compare Pro-tuning with one important baseline, denoted by Pro-tuning_{fine-tune}, in which our prompt blocks are trained together with the pre-trained vision model. As listed in Table 8, joint training of prompt blocks and the pre-trained vision model degrades performance compared with merely updating prompt blocks, closely to fine-tuning. This is reasonable since training the pre-trained model on downstream datasets may hurt its capability of general-purpose visual modeling, due to the much less number of downstream images compared with the large-scale dataset used for pre-training, where the similar phenomena also occur in the vision-language model [20; 48].

Table 8: Validation accuracy comparisons of Pro-tuning and other tuning settings on long-tailed CIFAR-100 with imbalanced ratio 100 under ResNet-50.

Methods	Training from scratch	Head retraining	Fine-tuning	Pro-tuning	Pro-tuning _{fine-tune}
Params (M)	23.71	0.20	23.71	3.82	27.33
Top-1 Acc. (%)	42.6	56.1	60.5	61.2	60.4

Impact of the capacity of prompt blocks. To investigate the influence of the capacity of prompt blocks, we compare Pro-tuning with its variants that use two prompt blocks or three prompt blocks on CIFAR-100 and long-tailed CIFAR-100 with imbalanced ratio 100 under ResNet-50. As listed in Table 9, we can observe that the increase of prompt blocks brings little help to transferability. This adequately validates that our Pro-tuning suffices to bring a significant performance gain only using one prompt block comprised of three convolutional layers. More results and analysis are provided in the supplementary material.

Table 9: Validation accuracy comparisons of different numbers of prompt blocks per stage on long-tailed CIFAR-100 with imbalanced ratio 100 under ResNet-50.

Dataset	#Block	#Params	Top-1 Acc.
CIFAR-100	1	3.82	83.6
	2	7.43	83.5
	3	11.05	83.7
CIFAR-100-LT-100	1	3.82	61.2
	2	7.43	61.3
	3	11.05	61.3

Influence of inserting positions. To evaluate the impact of inserting positions of prompt blocks, we model Pro-tuning with different inserting positions and numbers under DeiT-B. As listed in Table 10, we find that our adopted multi-stage inserting way achieves the best performance. Besides, it can be observed that only inserting after the first layer and our used uniformly inserting can obtain better generalization performance compared with only inserting after the last layer. A considerable reason is that low-level and mid-level semantics could be more significant than high-level semantics for

transferability, as pointed in [19; 53; 56]. More experimental results about inserting positions of prompt blocks are provided in the supplementary material.

Table 10: Influence of inserting position for prompt blocks on long-tailed CIFAR-100 with imbalanced ratio 100 under DeiT-B. “F1”: inserting a prompt block after the first transformer layer. “F5”: inserting five prompt blocks after the first transformer layer. “L1”: inserting a prompt block after the last transformer layer. “L5”: inserting five prompt blocks after the last transformer layer. “U5”: uniformly inserting four prompt blocks in 12 transformer layers along with one prompt block after the embedding layer, as our default setting.

Position	F1	F5	L1	L5	U5
Params (M)	0.69	3.17	0.69	3.17	3.17
Top-1 Acc. (%)	73.0	73.5	67.4	67.5	74.0

Effect of adaptive prompt. To evaluate the effect of adaptive prompt, we compare Pro-tuning under different settings for the ratio β in prompt blocks in Eq. (1) on long-tailed CIFAR-100 with imbalanced ratio 100 under ResNet-50. Specifically, we set β as a fixed constant or a learnable parameter. As listed in Table 11, one can observe that the learnable β achieves superior performance over all constants. This adequately validates the effectiveness of our adaptive prompt. Interestingly, we can find that the decreasing number of β consistently boosts performance varying from 10 to 0.1. This phenomenon implies that encouraging the feature representations from the pre-trained model may facilitate transferability when training Pro-tuning.

Table 11: Validation accuracy comparisons of different settings of β in prompt blocks in Eq. (1) on long-tailed CIFAR-100 with imbalanced ratio 100 under ResNet-50.

β	10	4	2	1	0.5	0.25	0.1	Lea.
Top-1 Acc.	50.3	49.7	49.5	51.8	53.2	54.4	56.6	58.1

Impact of different kernel sizes in prompt blocks. We evaluate Pro-tuning under the different kernel sizes k of the second convolution in prompt blocks on CIFAR-100 and long-tailed CIFAR-100 with imbalanced ratio 100 under ResNet-50. The results in Table 12 indicate that our Pro-tuning performs outstanding transferability under diverse kernel sizes. Additionally, the performance generally improves with the increase of kernel size, then the performance will saturate when the kernel size $k = 5$ is satisfied. A considerable reason is that the increase of receptive field size typically enhances the representation ability. Nevertheless, a quite large kernel size results in difficult optimization, hence there is little benefit from a larger kernel size. Thus, we set the kernel size as 5 in our experiments unless specified otherwise.

Table 12: Validation accuracy comparisons of different kernel sizes in prompt blocks on long-tailed CIFAR-100 with imbalanced ratio 100 under ResNet-50.

Dataset	#Kernel	#Params	Top-1 Acc.
CIFAR-100	3	3.76	83.2
	5	3.82	83.6
	7	3.91	83.4
CIFAR-100-LT-100	3	3.67	60.9
	5	3.82	61.2
	7	3.91	61.1

5 Discussion

In our view, the significant performance gain of the proposed Pro-tuning could be attributed to its capability of modeling the task-specific prior for the latent manifold of image data. Essentially, the pre-trained vision model learns a data manifold. When various perturbations occur on a downstream dataset, the downstream data will deviate from the learned data manifold. To alleviate this problem, traditional transfer methods typically finetune the whole learned data manifold on the downstream dataset. However, due to a limited amount of downstream data, this way is prone to 1) overfitting on the downstream dataset; 2) extreme difficulty in optimization, as the learned data manifold could be a fine-detailed structure with high-level semantics. By learning a task-specific prior, our Pro-tuning can guide the deviated downstream data back to the learned manifold, thus avoiding the performance drop of the pre-trained model on downstream tasks.

6 Conclusion

In this work, we present Pro-tuning, a parameter-efficient vision tuning paradigm by extending the prompt-based philosophy to pre-trained vision models. The main idea of Pro-tuning is to maximally mitigate the gap between pre-training and tuning on downstream tasks by adapting the feature distribution of the pre-trained model at various levels. To this end, we propose multiple stage-wise prompt blocks, which can be simply plugged into given frozen pre-trained models, *e.g.*, CNNs and vision transformers. Extensive experiments on fifteen challenging vision datasets have demonstrated the effectiveness and generalizability of our method.

Further work may include applying vision prompt to other computer vision tasks, such as object detection and semantic segmentation. Our work, as well as recent vision-language models, show the promise of this extension, but how to efficiently devise vision prompt for these pixel-level dense predictions remains to be solved.

Limitation. The limitations of Pro-tuning are mainly three aspects: 1) it is applicable in settings where the categories lie in a closed set; 2) it relies on a strong pre-trained model; 3) the inference still has the full computational cost of pre-trained models, which may limit its development in the edge devices.

Broader impact. Our work paves the new road to applying the pre-trained vision models. It has a broad application prospect in the common scenarios, such as cloud services. However, the proposed method may be maliciously used to solve those downstream tasks of involving damage peoples' livelihood or economic security, such as privacy theft and economic fraud. This issue warrants further consideration when this work is deployed in publicly available platforms such as cloud services.

References

- [1] P. Agrawal, R. Girshick, and J. Malik. Analyzing the performance of multilayer neural networks for object recognition. In *ECCV*, pages 329–344, 2014.
- [2] P. Anderson, X. He, C. Buehler, D. Teney, M. Johnson, S. Gould, and L. Zhang. Bottom-up and top-down attention for image captioning and visual question answering. In *CVPR*, pages 6077–6086, 2018.
- [3] T.B. Brown, B. Mann, N. Ryder, M. Subbiah, J. Kaplan, P. Dhariwal, A. Neelakantan, P. Shyam, G. Sastry, A. Askell, et al. Language models are few-shot learners. In *NeurIPS*, pages 1877–1901, 2020.
- [4] Z. Cai and N. Vasconcelos. Cascade r-cnn: high quality object detection and instance segmentation. *IEEE TPAMI*, 43(5):1483–1498, 2019.
- [5] K. Cao, C. Wei, A. Gaidon, N. Arechiga, and T. Ma. Learning imbalanced datasets with label-distribution-aware margin loss. In *NeurIPS*, pages 1565–1576, 2019.
- [6] K. Chen, J. Pang, J. Wang, Y. Xiong, X. Li, S. Sun, W. Feng, Z. Liu, J. Shi, W. Ouyang, et al. Hybrid task cascade for instance segmentation. In *CVPR*, pages 4974–4983, 2019.
- [7] X. Chen, S. Wang, B. Fu, M. Long, and J. Wang. Catastrophic forgetting meets negative transfer: Batch spectral shrinkage for safe transfer learning. In *NeurIPS*, pages 1906–1916, 2019.
- [8] F. Chollet. Xception: Deep learning with depthwise separable convolutions. In *CVPR*, pages 1251–1258, 2017.
- [9] J. Deng, W. Dong, R. Socher, L. Li, K. Li, and F. Li. Imagenet: A large-scale hierarchical image database. In *CVPR*, 2009.
- [10] J. Donahue, Y. Jia, O. Vinyals, J. Hoffman, N. Zhang, E. Tzeng, and T. Darrell. Decaf: A deep convolutional activation feature for generic visual recognition. In *ICML*, pages 647–655, 2014.
- [11] P. Gao, S. Geng, R. Zhang, T. Ma, R. Fang, Y. Zhang, H. Li, and Y. Qiao. Clip-adapter: Better vision-language models with feature adapters. *arXiv preprint arXiv:2110.04544*, 2021.
- [12] T. Gao, A. Fisch, and D. Chen. Making pre-trained language models better few-shot learners. In *ACL*, pages 3816–3830, 2021.

- [13] K. He, X. Zhang, S. Ren, and J. Sun. Deep residual learning for image recognition. In *CVPR*, pages 770–778, 2016.
- [14] D. Hendrycks, S. Basart, N. Mu, S. Kadavath, F. Wang, E. Dorundo, R. Desai, T. Zhu, S. Parajuli, M. Guo, et al. The many faces of robustness: A critical analysis of out-of-distribution generalization. In *ICCV*, pages 8340–8349, 2021.
- [15] D. Hendrycks and T. Dietterich. Benchmarking neural network robustness to common corruptions and perturbations. In *ICLR*, 2019.
- [16] D. Hendrycks, K. Zhao, S. Basart, J. Steinhardt, and D. Song. Natural adversarial examples. In *CVPR*, pages 15262–15271, 2021.
- [17] N. Houlsby, A. Giurgiu, S. Jastrzebski, B. Morrone, De L.Q., A. Gesmundo, M. Attariyan, and S. Gelly. Parameter-efficient transfer learning for nlp. In *ICML*, pages 2790–2799, 2019.
- [18] J. Hu, L. Shen, and G. Sun. Squeeze-and-excitation networks. In *CVPR*, pages 7132–7141, 2018.
- [19] A. Islam, C. Richard. Chen, R. Panda, L. Karlinsky, R. Radke, and R. Feris. A broad study on the transferability of visual representations with contrastive learning. In *ICCV*, pages 8845–8855, 2021.
- [20] C. Jia, Y. Yang, Y. Xia, Y. Chen, Z. Parekh, H. Pham, Q.V. Le, Y. Sung, Z. Li, and T. Duerig. Scaling up visual and vision-language representation learning with noisy text supervision. In *ICML*, pages 4904–4916, 2021.
- [21] A. Kamath, M. Singh, Y. LeCun, G. Synnaeve, I. Misra, and N. Carion. Mdetr-modulated detection for end-to-end multi-modal understanding. In *ICCV*, pages 1780–1790, 2021.
- [22] A. Khosla, N. Jayadevaprakash, B. Yao, and F. Li. Novel dataset for fine-grained image categorization: Stanford dogs. In *CVPR Workshop*, 2011.
- [23] S. Kornblith, J. Shlens, and Q.V. Le. Do better imagenet models transfer better? In *CVPR*, pages 2661–2671, 2019.
- [24] Alex Krizhevsky, Geoffrey Hinton, et al. Learning multiple layers of features from tiny images. 2009.
- [25] B. Lester, R. Al-Rfou, and N. Constant. The power of scale for parameter-efficient prompt tuning. In *EMNLP*, 2021.
- [26] F. Li, Rob Fergus, and Pietro Perona. Learning generative visual models from few training examples: An incremental bayesian approach tested on 101 object categories. In *CVPR Workshop*, pages 178–178, 2004.
- [27] X. Li, H. Xiong, H. Wang, Y. Rao, L. Liu, Z. Chen, and J. Huan. Delta: Deep learning transfer using feature map with attention for convolutional networks. In *ICLR*, 2019.
- [28] X.L. Li and P. Liang. Prefix-tuning: Optimizing continuous prompts for generation. In *ACL/IJCNLP*, 2021.
- [29] G. Lin, A. Milan, C. Shen, and I. Reid. Refinenet: Multi-path refinement networks for high-resolution semantic segmentation. In *Proceedings of the IEEE conference on computer vision and pattern recognition*, pages 1925–1934, 2017.
- [30] T. Lin, P. Dollár, R. Girshick, K. He, B. Hariharan, and S. Belongie. Feature pyramid networks for object detection. In *CVPR*, pages 2117–2125, 2017.
- [31] Tsung-Yi Lin, Michael Maire, Serge Belongie, James Hays, Pietro Perona, Deva Ramanan, Piotr Dollár, and C Lawrence Zitnick. Microsoft coco: Common objects in context. In *European conference on computer vision*, pages 740–755, 2014.
- [32] Z. Lin, A. Madotto, and P. Fung. Exploring versatile generative language model via parameter-efficient transfer learning. In *EMNLP*, pages 441–459, 2020.

- [33] P. Liu, W. Yuan, J. Fu, Z. Jiang, H. Hayashi, and G. Neubig. Pre-train, prompt, and predict: A systematic survey of prompting methods in natural language processing. *arXiv preprint arXiv:2107.13586*, 2021.
- [34] Z. Liu, Y. Lin, Y. Cao, H. Hu, Y. Wei, Z. Zhang, S. Lin, and B. Guo. Swin transformer: Hierarchical vision transformer using shifted windows. In *ICCV*, pages 10012–10022, 2021.
- [35] J. Long, E. Shelhamer, and T. Darrell. Fully convolutional networks for semantic segmentation. In *CVPR*, pages 3431–3440, 2015.
- [36] M.E. Nilsback and A. Zisserman. Automated flower classification over a large number of classes. In *ICVGIP*, pages 722–729, 2008.
- [37] O.M. Parkhi, A. Vedaldi, A. Zisserman, and CV Jawahar. Cats and dogs. In *CVPR*, pages 3498–3505, 2012.
- [38] F. Petroni, T. Rocktäschel, P. Lewis, A. Bakhtin, Y. Wu, A.H. Miller, and S. Riedel. Language models as knowledge bases? In *EMNLP*, pages 2463–2473, 2019.
- [39] J. Pfeiffer, A. Kamath, A. Rücklé, K. Cho, and I. Gurevych. Adapterfusion: Non-destructive task composition for transfer learning. *arXiv preprint arXiv:2005.00247*, 2020.
- [40] A. Radford, J.W. Kim, C. Hallacy, A. Ramesh, G. Goh, S. Agarwal, G. Sastry, A. Askell, P. Mishkin, J. Clark, et al. Learning transferable visual models from natural language supervision. In *ICML*, pages 8748–8763, 2021.
- [41] A. Radford, K. Narasimhan, T. Salimans, and I. Sutskever. Improving language understanding by generative pre-training. 2018.
- [42] A. Radford, J. Wu, R. Child, D. Luan, D. Amodei, I. Sutskever, et al. Language models are unsupervised multitask learners. *OpenAI blog*, 1(8):9, 2019.
- [43] I. Radosavovic, R.P. Kosaraju, R. Girshick, K. He, and P. Dollár. Designing network design spaces. In *CVPR*, pages 10428–10436, 2020.
- [44] S.A. Rebuffi, H. Bilen, and A. Vedaldi. Learning multiple visual domains with residual adapters. In *NeurIPS*, pages 506–516, 2017.
- [45] T. Schick and H. Schütze. Exploiting cloze questions for few shot text classification and natural language inference. In *EACL*, pages 255–269, 2020.
- [46] Alon Talmor, Yanai Elazar, Yoav Goldberg, and Jonathan Berant. olympics-on what language model pre-training captures. *TACL*, 8:743–758, 2020.
- [47] H. Touvron, M. Cord, M. Douze, F. Massa, A. Sablayrolles, and H. Jégou. Training data-efficient image transformers & distillation through attention. In *ICML*, pages 10347–10357, 2021.
- [48] M. Tsimpoukelli, J. Menick, S. Cabi, S. Eslami, O. Vinyals, and F. Hill. Multimodal few-shot learning with frozen language models. *arXiv preprint arXiv:2106.13884*, 2021.
- [49] O. Vinyals, A. Toshev, S. Bengio, and D. Erhan. Show and tell: A neural image caption generator. In *CVPR*, pages 3156–3164, 2015.
- [50] T. Xiao, Y. Liu, B. Zhou, Y. Jiang, and J. Sun. Unified perceptual parsing for scene understanding. In *ECCV*, pages 418–434, 2018.
- [51] T. Xiao, T. Xia, Y. Yang, C. Huang, and X. Wang. Learning from massive noisy labeled data for image classification. In *CVPR*, pages 2691–2699, 2015.
- [52] L. Xuhong, Y. Grandvalet, and F. Davoine. Explicit inductive bias for transfer learning with convolutional networks. In *ICML*, pages 2825–2834, 2018.
- [53] J. Yosinski, J. Clune, Y. Bengio, and H. Lipson. How transferable are features in deep neural networks? pages 3320–3328, 2014.

- [54] K. You, Z. Kou, M. Long, and J. Wang. Co-tuning for transfer learning. In *NeurIPS*, pages 17236–17246, 2020.
- [55] K. You, Y. Liu, J. Wang, and M. Long. Logme: Practical assessment of pre-trained models for transfer learning. In *ICML*, pages 12133–12143, 2021.
- [56] N. Zhao, Z. Wu, R.WH. Lau, and S. Lin. What makes instance discrimination good for transfer learning? *arXiv preprint arXiv:2006.06606*, 2020.
- [57] B. Zhou, H. Zhao, X. Puig, S. Fidler, A. Barriuso, and A. Torralba. Scene parsing through ade20k dataset. In *CVPR*, pages 633–641, 2017.
- [58] K. Zhou, J. Yang, C.C. Loy, and Z. Liu. Learning to prompt for vision-language models. *arXiv preprint arXiv:2109.01134*, 2021.